Cantilever array sensors

by Hans Peter Lang[1,2*], Martin Hegner[1], and Christoph Gerber[1]

Miniaturized microfabricated sensors have enormous potential in gas detection, biochemical analysis, medical applications, quality and process control, and product authenticity issues. Here, we highlight an ultrasensitive mechanical way of converting (bio-)chemical or physical processes into a recordable signal using microfabricated cantilever arrays.

Cantilevers are typically rectangular-shaped bars of Si less than 1 μm thick. Adsorption/recognition of molecules on the surface of such micromechanical cantilevers functionalized with receptor molecules results in bending of the cantilever because of the surface stress. The bending is detected by deflection of a laser beam. Cantilever sensors can be operated in various environments, such as vacuum, air, or liquids. The major advantages of such miniaturized sensors are their small size, fast response times, high sensitivity, and direct transduction without the need for any labels.

Microfabricated cantilevers are mainly used as force sensors to image the topography of a surface by means of techniques such as scanning force microscopy (SFM) or atomic force microscopy (AFM)[1,2]. In these methods (Fig. 1), a cantilever with a sharp tip is scanned across a conductive or nonconductive surface using an *x-y-z* actuator system (e.g. a piezoelectric scanner). The sample's surface is imaged in a rectangular or square pattern of parallel scan lines. The tip can be either in direct contact with the surface (contact mode) or oscillated to interact with the surface only for a short time during the oscillation cycle (dynamic, noncontact mode). The bending of the cantilever is usually measured via optical detection of the position of a laser beam deflected at the apex of a cantilever, or via piezoresistive strain gauges. The interaction of the cantilever tip with the surface is common to all SFM methods. This interaction may be used to control the feedback loop that maintains a constant force or force gradient between cantilever tip and sample surface.

[1]National Competence Center for Research (NCCR) in Nanoscale Science Basel,
Klingelbergstrasse 82,
CH-4056 Basel, Switzerland

[2]IBM Research, Zurich Research Laboratory,
Säumerstrasse 4,
CH-8803 Rüschlikon, Switzerland

*E-mail: Hans-Peter.Lang@unibas.ch

ISSN:1369 7021 © Elsevier Ltd 2005

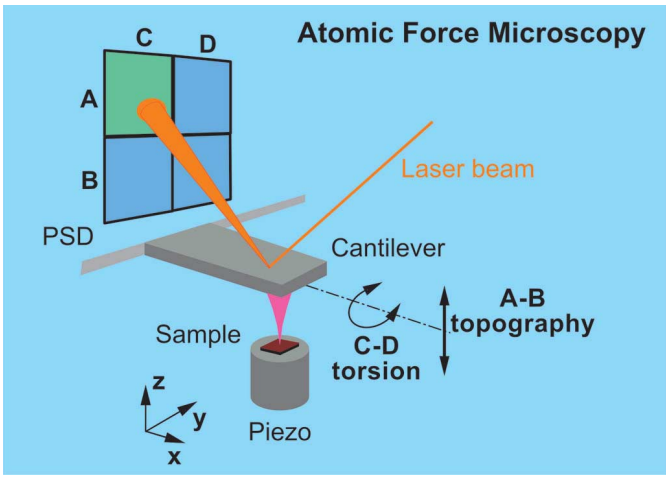

Fig. 1 Schematic of the atomic force microscopy technique. (Courtesy of Robert Sum, Liestal, Switzerland.)

By recording the correction signal applied to the *z*-actuation drive to keep the interaction between tip and sample surface constant, a topography image of the sample surface is obtained. AFM has developed into the most powerful and versatile surface-characterization tool of today to investigate surfaces at the molecular and atomic level.

These methods are well established and widely used. In this review, however, we focus on applications of cantilevers beyond the imaging of surfaces.

Principles of operation

For sensing purposes neither a sharp tip nor a sample surface is required. We simply use an array of eight cantilever beams, each coated with a sensitive layer for molecular recognition (Fig. 2)[3]. Such devices represent ultrasensitive

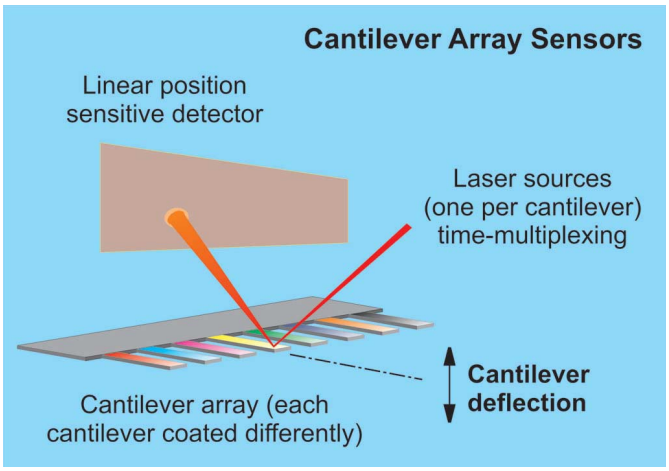

Fig. 2 Schematic of the cantilever-array sensor readout. Different sensing layers are shown in different colors.

nanomechanical sensors for the detection of chemical and biochemical reactions in both gas-phase and liquid environments[4-15]. The sensitive layer can be either highly specific for molecular recognition or only partially specific to produce response patterns for various analytes, provided that each of the cantilevers is coated with a different partially specific sensor layer. In a gaseous environment, this configuration may be used as an artificial nose to characterize volatile vapors and odors[3,16-19].

In liquid, the cantilever sensors allow rapid, quantitative, and qualitative detection of nonlabeled biomolecules, e.g. for sequence-specific DNA hybridization with single-base mismatch sensitivity or for molecular recognition (such as antibody-antigen interactions and protein-protein recognition)[20-24].

Cantilever sensors can be operated in static, dynamic, and heat modes (Fig. 3)[8,22,23,25]. In static mode[9,20,26], the mechanical response of a sensitive layer applied onto one cantilever surface (e.g. the upper one) to the adsorption or recognition of molecules from the environment produces a signal. The surface stress occurring during the adsorption process results in a static bending of the cantilever. Surface stresses of several 10^{-3} N/m result in deflections of about 10 nm for the cantilever sensors used here[21].

In dynamic mode[6,7,19], the cantilever is oscillated externally at its resonance frequency using a piezoelectric actuator. The cantilever may be coated on its upper and lower surfaces with a molecular layer sensitized to recognize molecules from the environment. On adsorption of mass on the cantilever, the resonance frequency is shifted to a lower value. From the shift in frequency, the adsorbed mass on the cantilever can be calculated[6,7,27,28], provided that the mechanical properties of the cantilever do not change significantly because of the adsorbed mass. A change of 1 Hz in resonance frequency roughly corresponds to a mass change of 1 pg for the cantilever sensors described here[19].

In heat (bimetallic) mode[4,5,8,25], the difference in the linear expansion coefficients of the cantilever material, e.g. single-crystalline Si typically with a 100 nm thick metallic

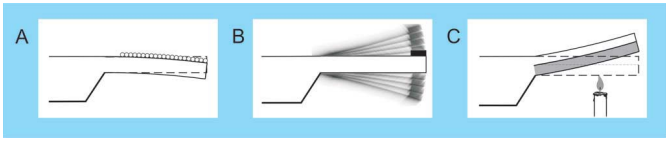

Fig. 3 Cantilever sensor operating modes: (A) static deflection mode; (B) dynamic resonance mode; and (C) bimetallic heat mode.

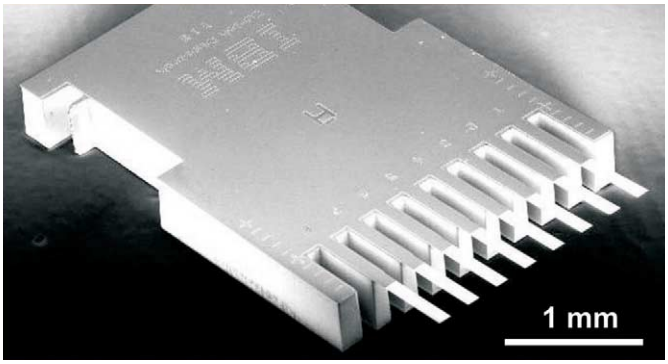

Fig. 4 Scanning electron micrograph of a cantilever sensor array. (Courtesy of Viola Barwich, University of Basel, Switzerland.)

layer applied to one of the surfaces, causes bending of the cantilever sensor if the temperature is changed. Temperature changes of 10^{-5} K produce cantilever deflections of several nanometers, which can be measured easily.

Piezoresistive microcantilever arrays are also used for actuation and for storage applications[29]. However, this is beyond the scope of this review.

Measurement setup

Si cantilever sensor arrays are microfabricated using a dry-etching silicon-on-insulator (SOI) fabrication technique developed in the Micro-/Nanomechanics Department at IBM's Zurich Research Laboratory. One chip comprises eight cantilevers, each 500 µm long, 100 µm wide, and 0.5 µm thick, arranged at a pitch of 250 µm. The resonance frequencies of the cantilevers vary by only 0.5%, demonstrating the high reproducibility and precision of the cantilever fabrication. A scanning electron micrograph of a cantilever sensor array chip is shown in Fig. 4.

The upper surface of these cantilevers is generally coated with 2 nm of Ti and 20 nm of Au to provide a reflective surface and an interface for attaching functional groups of probe molecules. For example, molecules with a thiol group can be anchored to the Au surface of the cantilever. Such thin metal layers are believed not to contribute significantly to the bending resulting from surface-stress changes because the temperature is kept constant. Many examples of molecular adsorption on cantilevers are described in the literature, for example the adsorption of alkyl thiols on Au[9], the pH-dependent response of carboxy-terminated alkyl thiols[26], and biomolecular recognition[20,21].

Fig. 5 shows the schematic setup of the experiments in (A) a gaseous and (B) a liquid (biochemical) environment. The cantilever sensor array is located in an analysis chamber of 3-90 µl in volume, which has inlet and outlet ports for gases or liquids. The cantilever deflection is determined via an array of eight vertical-cavity surface-emitting lasers (VCSELs) arranged at a linear pitch of 250 µm that emit at a wavelength of 760 nm into a cone of 5-10°. A time-multiplexing procedure switches the lasers on and off sequentially. The light of each VCSEL is collimated and focused onto the apex of the corresponding cantilever. The light is then reflected off the Au-coated surface of the cantilever and impinges on the surface of a position-sensitive detector (PSD). PSDs are photopotentiometer-like, light-sensitive devices that produce photocurrents at two opposing electrodes. These allow the position of an incident light beam to be determined with micrometer precision. The photocurrents are transformed into voltages and amplified by a preamplifier. The resulting deflection signal is digitized and stored together with time information on a computer, which also controls the multiplexing of the VCSELs, the switching of the valves, and the mass flow controllers used to set the composition ratio of the analyte mixture.

The setup for measurements of liquids (Fig. 5B) consists of a polyetheretherketone (PEEK) liquid cell, which contains the

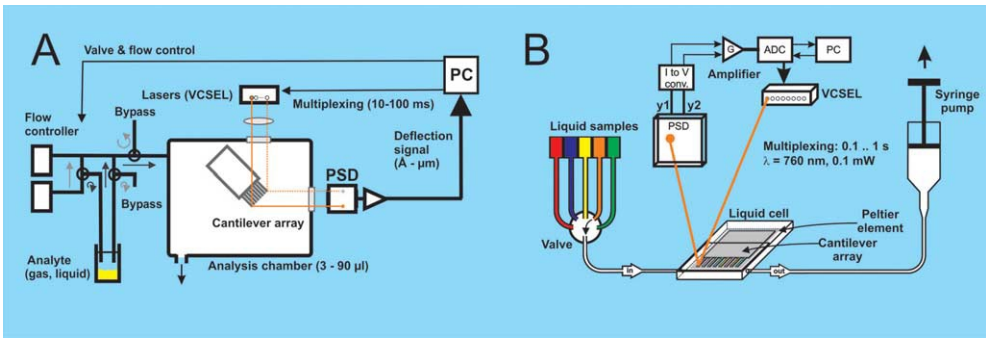

Fig. 5 Schematic of measurement setups for (A) a gaseous (artificial nose) and (B) a liquid environment (biochemical sensor).

cantilever array and is sealed by a Viton® O-ring and a glass plate. The VCSELs and the PSD are mounted on a metal frame around the liquid cell. After preprocessing the position of the deflected light beam in a current-to-voltage converter and amplifier stage, the signal is digitized in an analog-to-digital converter and stored on a computer. The liquid cell is equipped with inlet and outlet ports for liquids. The biochemical liquid samples are stored in individual, thermally equilibrated glass containers. A six-position valve allows the inlet to the liquid chamber to be connected to each of the liquid sample containers separately. The liquids are pulled through the liquid chamber by means of a syringe pump connected to the outlet of the chamber. A peltier element is situated very close to the lumen of the chamber to allow temperature regulation within the chamber. The entire setup is housed in a temperature-controlled box regulated with an accuracy of 0.01 K to the target temperature.

Cantilever functionalization and measurement process

Cantilever coatings can be applied by various techniques, such as incubation in dimension-matched glass capillaries or coating using an ink-jet spotting device (Fig. 6). For functionalization of the upper cantilever surface for gas-phase environment measurements, various commercial polymers are dissolved in solvents (5 mg/ml). Eight droplets of solution are dispensed onto the upper surface of one of the cantilevers of the array by ink-jet spotting[30,31] (Fig. 6A), allowed to dry, and form a homogeneous polymer layer of a few hundred nanometers thick.

Analyte vapor detection proceeds via the following mechanism. Target analyte molecules, e.g. from solvent vapors, are introduced into the measurement chamber and diffuse into the polymer layer on the cantilever surface. This diffusion process results in swelling of the polymer. The swelling bends the cantilevers in a way that is specific to the interaction between solvent vapor and polymer in terms of the magnitude of the bending and the temporal evolution. The resulting bending pattern is evaluated using principal-component analysis (PCA) techniques[32].

For measurements in the liquid phase, functional monolayers are generally applied by self-assembly of thiolated molecular layers, e.g. DNA oligonucleotide layers for hybridization experiments. Various oligonucleotide layers are applied in parallel using microcapillaries under identical

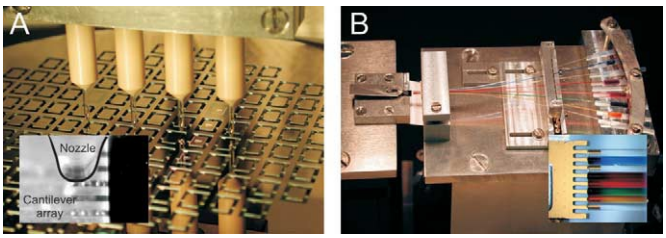

Fig. 6 Cantilever array functionalization using (A) a four-nozzle ink-jet device (the inset shows spotted liquid droplets at the upper surface of the cantilever) and (B) an array of eight microcapillaries (the inset shows how the individual cantilevers of the array are inserted into the array of microcapillaries; the colored liquids are for visualization purposes only). (Courtesy of Alexander Bietsch, University of Basel, Switzerland.)

conditions to the individual cantilever sensors and filled with a 40 μM solution of 3'- or 5'-thiolated probe DNA in triethyl ammonium acetate buffer for 20 min (Fig. 6B). The coated arrays are rinsed in sodium saline citrate (ssc) 5x buffer and dried in nitrogen[21].

Artificial nose applications

A cantilever array with eight differently coated cantilevers can be applied as an artificial nose to characterize vapors. An artificial nose consists of an array of chemical sensors with partial specificity and an appropriate pattern-recognition system to recognize simple or complex odors[33]. It involves a sensor array, a pattern classifier, and a sampling system to perform measurements reproducibly. The sensor array is exposed to the same sample and produces individual responses as well as a pattern of responses. A single chemical sensor consists of a physical transducer and a chemical interface layer or a receptor domain. The main advantages of an artificial nose is that it is reproducible, does not fatigue, and can be placed in environments harmful to human beings.

Here we use polymer-coated cantilevers as chemical sensors prepared as described above. Detection of vapors proceeds via diffusion of the vapor molecules into the polymer, resulting in swelling of the polymer and bending of the cantilever. The bending is specific to the interaction between the solvent vapor and polymer in terms of time and magnitude. To demonstrate the capability of the cantilever-array artificial nose, we injected vapor (20 ml/min) from the headspace above 0.1 ml of ethanolic solution of perfume essence samples in a stream of dry nitrogen. Fig. 7A shows the deflection traces from eight polymer-coated cantilevers upon injection of perfume essence vapor over 60 s (starting at t = 100 s). After injection, the bending signal increases because of the swelling of the polymer. The pattern-

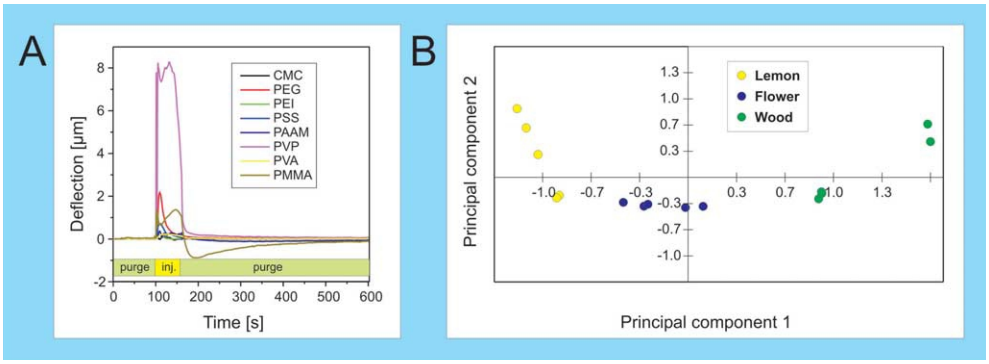

Fig. 7 (A) Bending pattern of polymer-coated cantilever sensors upon exposure to wood perfume essence vapor. The abbreviations of polymers (all concentrations 5 mg/ml) denote: CMC – carboxy methyl cellulose sodium salt in water; PEG – polyethylene glycol, molecular weight (MW) 6000 in water; PEI – polyethyleneimine in water; PSS – poly(sodium 4-styrene sulfonate), MW 70 000 in water; PAAM – poly(allylamine hydrochloride), MW 15 000 in water; PVP – poly(2-vinylpyridine) standard, MW 64 000 in ethanol; PVA – polyvinylalcohol 10-98 in dimethylsulfoxide; PMMA – polymethyl methacrylate, MW 15 000 in methyl-isobutyl-ketone. 'Purge' means flushing the measurement chamber with dry nitrogen gas at a rate of 20 ml/min, 'Inj.' denotes the injection of dry nitrogen gas saturated with the vapor from the headspace of a vial filled with 100 µl of ethanolic solution of perfume essence. (B) PCA plot of perfume essence samples. Measurements of flower, wood, and lemon perfume essence can be distinguished easily and reproducibly.

recognition system uses the magnitudes of deflection of all eight cantilevers at three points in time (after 110 s, 130 s, and 150 s) as input, thus describing the diffusion process of molecules into the polymer layer. This procedure yields a set of 8 × 3 = 24 cantilever magnitudes, representing a so-called 'fingerprint' of the perfume essence vapor (partial specificity of the chemical sensors). The data are transformed and projected using PCA algorithms. PCA extracts the predominant peculiarities in responses for various vapors. The largest differences in signal amplitudes of the fingerprint patterns are plotted in a two-dimensional graph. An individual experiment (i.e. a set of 24 cantilever magnitudes) represents a single point in the PCA space. The axes refer to projections of the multidimensional datasets into two dimensions (principal components). This procedure is aimed at maximum distinction performance between vapors, i.e. several measurements of the same vapor should yield a cluster of points in principal component space. Measurements of different vapors should produce well-separated clusters of points.

Samples of perfume essences (lemon, wood, and flower; main components: ethanol 35%, water 14%, dipropylene glycol 50%, fragrances <1%) have been used to demonstrate the separation selectivity of the cantilever-sensor setup. The PCA evaluation of the cantilever-sensor response curves is shown in Fig. 7B. Clear clustering is observed for the perfume essences tested, demonstrating the successful recognition and selectivity of the method. Note that the 'artificial nose' can only recognize sample vapors that have been measured before. Therefore, it is a characterization tool rather than a chemical analysis tool.

DNA hybridization measurements

The great advantage of cantilever array sensors is that measurements of differences in the responses of sensor and reference cantilevers can be evaluated. Measuring the deflection of only one cantilever will yield misleading results that might give rise to an incorrect interpretation of the cantilever deflection trace[23]. Therefore, at least one of the cantilevers (the sensor cantilever) is coated with a sensitive layer that exhibits an affinity to the molecules to be detected, while other cantilevers are coated with a molecular layer that does not show an affinity to the molecules to be detected (reference cantilevers).

The biochemical system investigated in this case involves a DNA hybridization experiment in liquid using a thiolated 12-mer oligonucleotide sequence from the Bio B biotin synthetase gene (EMBL accession number: J04423). We selected two surface-bound probes, Bio B1 (5'-SH-C6-ACA TTG TCG CAA-3', where C6 is a spacer) and Bio B2 (5'-SH-C6-TGC TGT TTG AAG-3'), which are immobilized by thiol binding onto the Au-coated upper surface of a cantilever in an array (Fig. 8A). The target complements, Bio B1C and

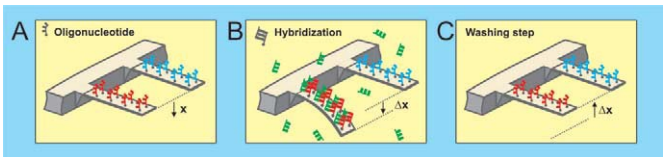

Fig. 8 Schematic of the cantilever-array DNA hybridization sensor. (A) Each cantilever is functionalized with a self-assembled monolayer of thiolated oligonucleotides. (B) Upon injection of the complementary sequence to the oligonucleotide sequence shown in front, hybridization takes place and the cantilever bends downwards. (C) After thorough rinsing with an unbinding agent, the cantilever in front returns to its initial position. (Schematics courtesy of Jürgen Fritz, currently at the International University of Bremen, Germany.)

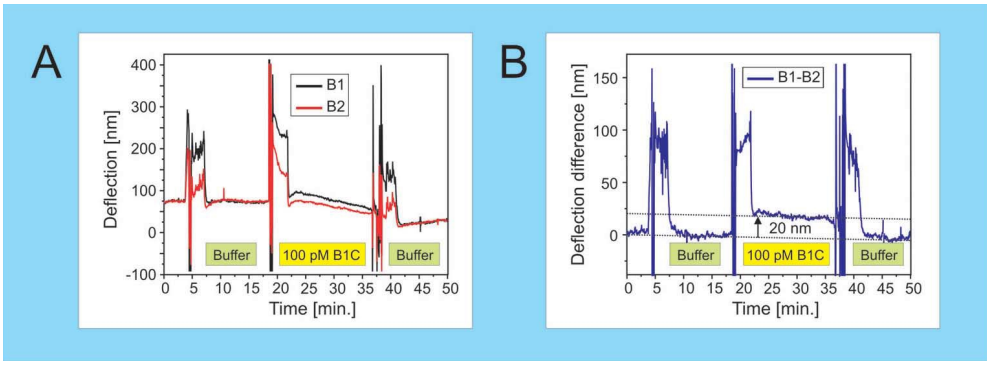

Fig. 9 (A) Deflection traces of sensor (functionalized with DNA oligonucleotide sequence Bio B1) and reference cantilevers (functionalized with DNA oligonucleotide sequence Bio B2). (B) Difference in the bending responses of the sensor cantilever B1 and reference cantilever B2. The dotted lines are guides to the eye. 'Buffer' indicates flushing the cell with 5x ssc buffer; '100 pM B1C' means injection of the complement to Bio B1 at a concentration of 100 pM in ssc buffer. (Data courtesy of Jiayun Zhang, University of Basel, Switzerland.)

Bio B2C, are diluted in 5x ssc buffer at 100 pM concentration. Upon injection of Bio B1C, the matching sequence to Bio B1, the sensor cantilever coated with Bio B1 will bend, whereas the reference cantilever coated with Bio B2 will not (Fig. 8B). After thorough rinsing with an unbinding agent, the cantilever coated with Bio B1 will bend back to its initial position (Fig. 8C). This bending is caused by the formation of surface stress during the hybridization process because of steric crowding (double-stranded DNA requires more space than single-stranded DNA).

The actual experiment was conducted as follows (Fig. 9A). First, the liquid cell with the functionalized cantilever array is filled with ssc buffer. After a stable baseline has been achieved (4 min), ssc buffer is injected for 3 min. The cantilevers deflect, but once the injection is completed, a stable baseline is reached again. At 18 min, the target Bio B1C is injected, which is supposed to hybridize with the Bio B1 probe, but not with the Bio B2 probe. Both cantilevers deflect, but the deflection magnitude of the Bio B1-coated cantilever is larger than that of the Bio B2-coated cantilever. Finally, at 37 min, ssc buffer is injected again and a stable baseline is reached. From the deflection data shown in Fig. 9A, it is clear that no conclusive result can be obtained from individual cantilever responses only, as both the sensor and the reference cantilever bend. However, a clear 20 nm deflection signal is observed when calculating the difference in deflection responses from probes Bio B1 (sensor) and reference Bio B2 (Fig. 9B). We conclude that it is mandatory to use at least two cantilevers in an experiment – a reference cantilever and a sensor cantilever – to be able to cancel out undesired artifacts such as thermal drift or unspecific adsorption.

Applications and outlook

The field of cantilever sensors has been very active in recent years[34,35]. The main topics in the 2004 literature include the following: detection of vapors and volatile compounds (e.g. HF vapor) using individual microcantilevers operated in beam deflection static mode[36-39]; gas-phase sensing applications for solvents using piezoresistive cantilevers[40-44]; biochemical applications in static mode in liquids[45-47] (e.g. as a glucose sensor); and C-reactive protein detection using dynamic-mode piezoresistive microcantilevers[48,49]. Several efforts have investigated the usability of microcantilever sensors as detectors for explosives[50-53] or *E. coli*[54,55]. A pH sensor using hydrogel coatings[56,57] has been suggested, as has the observation of electrochemical redox reactions using microcantilevers[58]. The theory of molecule adsorption on cantilevers has been investigated in several publications[59-63], whereas the bending, calibration, and curvature of cantilevers has been studied experimentally[64-66]. A new strategy to grow polymer brushes on the surface of microcantilevers has been proposed[67]. Others have described the production of polymer microcantilevers[68]. Torsional or lateral resonance modes could also be exploited for improved mass sensing in dynamic mode[69,70]. Nanowire electrodes attached to cantilevers in an array could be used for local multiprobe resistivity measurements[71], and two-dimensional microcantilever arrays have been suggested for multiplexed biomolecular analysis[72].

We conclude that cantilever sensor array techniques allow us to study physisorption and chemisorption processes, as well as determine material-specific properties such as enthalpy changes during phase transitions. Experiments in liquid environments have provided new insights into such complex biochemical reactions as the hybridization of DNA or

molecular recognition in antibody/antigen systems or proteomics. Our own current developments are toward technological applications, e.g. new ways to characterize real-world materials such as clinical blood samples. For example, the development of medical diagnostic tools will require improvement in the sensitivity of a large number of genetic tests that are performed with small amounts of single donor-blood or body-fluid samples. On the other hand, from a scientific point of view, the challenge lies in optimizing cantilever sensors to improve their sensitivity until the ultimate limit is reached, which may be the nanomechanical detection of individual molecules. MT

Acknowledgments

We thank U. Drechsler, M. Despont, R. Allenspach, and P. F. Seidler (IBM Research, Zurich Research Laboratory, Rüschlikon, Switzerland), as well as E. Meyer and H.-J. Güntherodt (University of Basel, Basel, Switzerland) for their continuous support. This project is funded partially by the National Center of Competence in Research in Nanoscience (Basel, Switzerland), the Swiss National Science Foundation, the Commission for Technology and Innovation (Bern, Switzerland), and IBM Research, Zurich Research Laboratory (Rüschlikon, Switzerland).

REFERENCES

1. Binning, G., *et al., Phys. Rev. Lett.* (1986) **56** (9), 930
2. Sarid, D., *Scanning Force Microscopy*, Oxford University Press, New York (1991)
3. Lang, H. P., *et al., Appl. Phys. Lett.* (1998) **72** (3), 383
4. Gimzewski, J. K., *et al., Chem. Phys. Lett.* (1994) **217** (5-6), 589
5. Barnes, J. R., *et al., Nature* (1994) **372**, 79
6. Thundat, T., *et al., Appl. Phys. Lett.* (1994) **64** (21), 2894
7. Wachter, E. A., and Thundat, T., *Rev. Sci. Instrum.* (1995) **66** (6), 3662
8. Berger, R., *et al., Microelectron. Eng.* (1997) **35** (1-4), 373
9. Berger, R., *et al., Science* (1997) **276**, 2021
10. Berger, R., *et al., Appl. Phys. A* (1998) **66** (Suppl. 1), S55
11. Scandella, L., *et al., Microporous Mesoporous Mater.* (1998) **21** (4-6), 403
12. Raiteri, R., *et al., Electrochim. Acta* (2000) **46** (6), 157
13. Moulin, A. M., *et al., Ultramicroscopy* (2000) **82** (1-4), 23
14. Craighead, H. G., *Science* (2000) **290**, 1532
15. Godin, M., *et al., Appl. Phys. Lett.* (2001) **79** (4), 551
16. Lang, H. P., *et al., Appl. Phys. A* (1998) **66** (Suppl. 1), S61
17. Lang, H. P., *et al., Anal. Chim. Acta* (1999) **393** (1-3), 59
18. Baller, M. K., *et al., Ultramicroscopy* (2000) **82** (1-4), 1
19. Battiston, F. M., *et al., Sens. Actuators, B* (2001) **77** (1-2), 122
20. Fritz, J., *et al., Science* (2000) **288**, 316
21. McKendry, R., *et al., Proc. Natl. Acad. Sci. USA* (2002) **99** (15), 9783
22. Lang, H. P., *et al., Chimia* (2002) **56**, 515
23. Lang, H. P., *et al., Nanotechnology* (2002) **13** (5), R29
24. Arntz, Y., *et al., Nanotechnology* (2003) **14** (1), 86
25. Berger, R., *et al., Chem. Phys. Lett.* (1998) **294** (4-5), 363
26. Fritz, J., *et al., Langmuir* (2000) **16** (25), 9694
27. Sader, J. E., *J. Appl. Phys.* (2001) **89** (5), 2911
28. Sader, J. E., *J. Appl. Phys.* (2002) **91** (11), 9354
29. Vettiger, P., *et al., Microelectron. Eng.* (1999) **46** (1-4), 11
30. Bietsch, A., *et al., Langmuir* (2004) **20** (12), 5119
31. Bietsch, A., *et al., Nanotechnology* (2004) **15** (8), 873
32. Timm, N. H., *Applied Multivariate Analysis*, Springer, Berlin, (2002)
33. Gardner, J., and Bartlett, P. N., (eds.), *Sensors and Sensory Systems for an Electronic Nose*, Kluwer Academic Publishers, Dordrecht (1992)
34. Lavrik, N. V., *et al., Rev. Sci. Instrum.* (2004) **75** (7), 2229
35. Ziegler, C., *Anal. Bioanal. Chem.* (2004) **379** (7-8), 946
36. Tang, Y., *et al., Anal. Chem.* (2004) **76** (9), 2478
37. Mertens, J., *et al., Sens. Actuators, B* (2004) **99** (1), 58
38. Yan, X. D., *et al., Instrum. Sci. Technol.* (2004) **32** (2), 175
39. Alvarez, M., *et al., Langmuir* (2004) **20** (22), 9663
40. Yum, K., *et al., J. Appl. Phys.* (2004) **96** (7), 3933
41. Kooser, A., *et al., Sens. Actuators, B* (2004) **99** (2-3), 474
42. Fadel, L., *et al., J. Micromech. Microeng.* (2004) **14** (9), S23
43. Fadel, L., *et al., Sens. Actuators, B* (2004) **102** (1), 73
44. Gunter, R. L., *et al., IEEE Sens. J.* (2004) **4** (4), 430
45. Pei, J. H., *et al., Anal. Chem.* (2004) **76** (2), 292
46. Yan, X., *et al., Chem. Phys. Lett.* (2004) **396** (1-3), 34
47. Zhang, Y., *et al., Biosens. Bioelectron.* (2004) **19** (11), 1473
48. Lee, J. H., *et al., Appl. Phys. Lett.* (2004) **84** (16), 3187
49. Lee, J. H., *et al., Biosens. Bioelectron.* (2004) **20** (2), 269
50. Pinnaduwage, L. A., *et al., Langmuir* (2004) **20** (7), 2690
51. Pinnaduwage, L. A., *et al., J. Appl. Phys.* (2004) **95** (10), 5871
52. Pinnaduwage, L. A., *et al., Sens. Actuators, B* (2004) **99** (2-3), 223
53. Pinnaduwage, L. A., *et al., Ultramicroscopy* (2004) **100** (3-4), 211
54. Zhang, J., and Ji, H.-F., *Anal. Sci.* (2004) **20**, 585
55. Gfeller, K. Y., *et al., Biosens. Bioelectron.* (2005), in press
56. Ke, L., and Ji, H.-F., *Anal. Sci.* (2004) **20**, 9
57. Zhang, Y. F., *et al., Instrum. Sci. Technol.* (2004) **32** (4), 361
58. Tian, F., *et al., Ultramicroscopy* (2004) **100** (3-4), 217
59. Bottomley, L., *et al., Anal. Chem.* (2004) **76** (19), 5685
60. Ryu, W. H., *et al., Sens. Actuators, B* (2004) **97** (1), 98
61. Ren, Q., and Zhao, Y.-P., *Microsyst. Technol.* (2004) **10** (2), 307
62. Khaled, A-R. A., and Vafai, K., *J. Micromech. Microeng.* (2004) **14** (8), 1220
63. Zhang, Y., *et al., J. Phys. D* (2004) **37** (15), 2140
64. Tang, Y. J., *et al., Sens. Actuators, B* (2004) **97** (1), 109
65. Hu, Z., *et al., Rev. Sci. Instrum.* (2004) **75** (2), 400
66. Jeon, S., and Thundat, T., *Appl. Phys. Lett.* (2004) **85** (6), 1083
67. Bambu, G.-G., *et al., Macromol. Chem. Phys.* (2004) **205** (13), 1713
68. McFarland, A. W., *et al., Rev. Sci. Instrum.* (2004) **75** (8), 2756
69. Ilic, B., *et al., J. Appl. Phys.* (2004) **95** (7), 3694
70. Sharos, L. B., *et al., Appl. Phys. Lett.* (2004) **84** (23), 4638
71. Lin, R., *et al., J. Appl. Phys.* (2004) **96** (5), 2895
72. Yue, M., *et al., J. Microelectromech. Syst.* (2004) **13** (2), 290